


RESEARCH PAPER

The natural compound, formononetin, extracted from *Astragalus membranaceus* increases adipocyte thermogenesis by modulating PPAR γ activity

Correspondence Donghai Wu, Key Laboratory of Regenerative Biology, Guangdong Provincial Key Laboratory of Stem Cell and Regenerative Medicine, Joint School of Life Sciences, Guangzhou Institutes of Biomedicine and Health, Chinese Academy of Sciences, Guangzhou 510530, China, and Tao Nie, Central Laboratory of the First Affiliated Hospital of Jinan University, Guangzhou 510630, China. E-mail: wu_donghai@gibh.ac.cn; nietaoly@126.com

Received 2 May 2017; **Revised** 26 November 2017; **Accepted** 1 December 2017

Tao Nie^{1,2,3,*} , Shiting Zhao^{2,3,*}, Liufeng Mao^{2,3,*}, Yiting Yang³, Wei Sun^{2,3}, Xiaoliang Lin⁴, Shuo Liu⁴, Kuai Li^{2,3}, Yirong Sun^{2,3}, Peng Li^{2,3}, Zhiguang Zhou⁵, Shaoqiang Lin¹, Xiaoyan Hui^{6,7}, Aimin Xu^{6,7}, Chung Wah Ma⁴, Yong Xu^{2,3}, Cunchuan Wang¹, P Rod Dunbar⁸ and Donghai Wu^{2,3,9}

¹Central Laboratory of the First Affiliated Hospital of Jinan University, Guangzhou, China, ²Key Laboratory of Regenerative Biology, Guangdong Provincial Key Laboratory of Stem Cell and Regenerative Medicine, Joint School of Life Sciences, Guangzhou Institutes of Biomedicine and Health, Chinese Academy of Sciences, Guangzhou, China, ³Guangzhou Medical University, Guangzhou, China, ⁴Research and Development Centre, Infinitus (China) Company Ltd., Guangzhou, China, ⁵Institute of Metabolism and Endocrinology, 2nd Xiangya Hospital, Central South University, Diabetes Center, Key Laboratory of Diabetes Immunology, Ministry of Education, National Clinical Research Center for Metabolic Diseases, Changsha, Hunan China, ⁶State Key Laboratory of Pharmaceutical Biotechnology, The University of Hong Kong, Hong Kong, Hong Kong, ⁷Department of Medicine, The University of Hong Kong, Hong Kong, Hong Kong, ⁸School of Biological Sciences and Maurice Wilkins Centre, University of Auckland, Auckland, New Zealand, and ⁹GUANGZHOU Regenerative Medicine and Health Laboratory, Guangzhou Institutes of Biomedicine and Health, Chinese Academy of Sciences, Guangzhou, China

*These authors contributed equally.

BACKGROUND AND PURPOSE

Increasing energy expenditure through adipocyte thermogenesis is generally accepted as a promising strategy to mitigate obesity and its related diseases. However, few clinically effective and safe agents are known to promote adipocyte thermogenesis. In this study, 20 traditional Chinese herbal medicines were screened to examine whether they induced adipocyte thermogenesis.

EXPERIMENTAL APPROACH

The effects of Chinese herbal medicines or components isolated from extracts of *A. membranaceus*, on adipocyte thermogenesis were analysed by assessing expression of uncoupling protein 1 (UCP1) by qPCR. Eight-week-old C57BL6/J male mice were fed a high-fat diet for 8 weeks and then randomized to two groups treated with vehicle or formononetin for another 8 weeks. Glucose tolerance tests and staining of adipose tissue with haematoxylin and eosin were carried out. Whole-body oxygen consumption was measured with an open-circuit indirect calorimetry system.

KEY RESULTS

Extracts of *A. membranaceus* increased expression of *Ucp1* in primary cultures of mouse adipocytes. Formononetin was the only known component of *A. membranaceus* extracts to increase adipocyte *Ucp1* expression. Diet-induced obese mice treated with formononetin gained less weight and showed higher energy expenditure than untreated mice. In addition, formononetin binds directly with PPAR γ .

CONCLUSIONS AND IMPLICATION

Taken together, our study demonstrates that the Chinese herbal medicine from *A. membranaceus* and its constituent formononetin have the potential to reduce obesity and associated metabolic disorders. Our results suggest that formononetin regulates adipocyte thermogenesis as a non-classical PPAR γ agonist.

Abbreviations

BAT, brown adipose tissue; LBD, ligand binding domain; UCP1, uncoupling protein 1; WAT, white adipose tissue

Introduction

Obesity is increasing worldwide, leading to numerous metabolic diseases (Di Cesare *et al.*, 2016). As energy imbalance is the main cause of obesity, it is effective to treat obesity by reducing energy intake or increasing energy expenditure. The uncoupling protein 1 (UCP1) can convert energy into heat thus increasing energy expenditure by non-shivering thermogenesis. As UCP1 is mainly expressed in the brown and brite/beige adipocytes, increasing UCP1 expression or activity in adipocytes is likely to provide a promising strategy to prevent and treat obesity (Feldmann *et al.*, 2009; Cypess *et al.*, 2013).

Brite/beige adipocytes can be induced in white adipose tissue (WAT) and their contribution to thermogenesis was estimated to equal to that of brown adipocytes (Shabalina *et al.*, 2014). The developmental origins of brown and beige adipocytes are different, but the underlying mechanism that regulates UCP1 expression is believed to be the same (Bartelt and Heeren, 2014). PPAR γ is a key transcriptional factor, regulating the expression of *Ucp1* by directly binding to its promoter (Villarroya *et al.*, 2007). Chronic activation of PPAR γ by its full agonist rosiglitazone can significantly induce UCP1 expression in primary epididymal adipocytes (Petrovic *et al.*, 2010). Rosiglitazone, but not the non-classical agonists of PPAR γ , can stabilize the critical co-activator protein PR domain containing 16 (PRDM16) to promote expression of *Ucp1* (Ohno *et al.*, 2010). PRDM16 not only determines the identity of brown fat cells but also controls the formation of beige adipocytes (Seale *et al.*, 2008; Cohen *et al.*, 2014).

Many cytokines or drugs have been demonstrated to treat obesity by increasing adipocyte thermogenesis, but a critical problem is that few people like to regard obesity as an illness and treat it medicinally (Buemann *et al.*, 2000; Fisher *et al.*, 2012; Bi *et al.*, 2014; Zhang *et al.*, 2014; Wang *et al.*, 2015; Baskaran *et al.*, 2016). Many traditional Chinese herbal medicines have been widely used to maintain daily health for hundreds of years. Therefore, 20 traditional Chinese herbal medicines were screened to examine whether they had the potential to induce adipocyte thermogenesis for the treatment of obesity. In this study, extracts of the plant *Astragalus membranaceus* and one component of the extracts, formononetin, were found to be involved in adipocyte thermogenesis *via* the regulation of PPAR γ activity.

Methods

Isolation of adipocytes and stromal vascular cells from adipose tissues

Adipose tissues were dissected from C57BL/6J mice, rinsed in phosphate-buffered saline, minced and digested for 40 min at

37°C in a 0.1% (w/v) type I collagenase solution (Sigma, Shanghai, China) with a D-Hanks buffer. The digested tissue was filtered through a 250 μ m nylon mesh and centrifuged at 800 \times g for 3 min. The sediment was resuspended in DMEM (Gibco, Guangzhou, China) with 10% FBS (HyClone, Guangzhou, China). Two days after reaching confluence (day 0), the cells were induced to differentiate into adipocytes in a medium containing 5 μ g \cdot mL $^{-1}$ insulin (Sigma), 1 μ M of dexamethasone (Sigma), 0.5 mM of isobutylmethylxanthine (IBMX; Calbiochem, Shanghai, China) and 1 μ M of rosiglitazone (Sigma). Two days later, the medium was replaced with DMEM supplemented with 10% FBS, 5 μ g \cdot mL $^{-1}$ of insulin and 1 μ M of rosiglitazone, and the cells were cultured for 6 days.

Chinese herbal medicine extracts

Dried roots of *A. membranaceus* (1kg dry weight) were added to 10 L of water and boiled for 2 h under reflux and then the first water extract was collected by filtration. The residue was added to 8000 mL of water and boiled for 1.5 h under reflux, and the second water extract obtained by filtration. The first and second water extracts were combined and concentrated to 500 mL by boiling and evaporation. As this final extract (500mL) was derived from 1kg of plant material, the concentration of this final extract is expressed as 2.0 g \cdot mL $^{-1}$ of *A. membranaceus*. The following Chinese herbal medicines were obtained by the same method: *Cichorium intybus* (1.5 g \cdot mL $^{-1}$), *Cinnamomum cassia* (0.3 g \cdot mL $^{-1}$), *Coix lachryma-jobi* (1.0 g \cdot mL $^{-1}$), *Zingiber officinale* (1 g \cdot mL $^{-1}$), *Eucommia ulmoides* (1.2 g \cdot mL $^{-1}$), *Eugenia caryophyllata* (0.2 g \cdot mL $^{-1}$), *Sophora japonica* (0.8 g \cdot mL $^{-1}$), *Hippophae rhamnoides* (0.42 g \cdot mL $^{-1}$), *Alpinia officinarum* (0.5 g \cdot mL $^{-1}$), *Lonicera japonica* (1 g \cdot mL $^{-1}$), *Morus alba* (1.2 g \cdot mL $^{-1}$), *Atractylodes lancea* (0.6 g \cdot mL $^{-1}$), *Lycium barbarum* (1.2 g \cdot mL $^{-1}$), *Piper nigrum* (0.1 g \cdot mL $^{-1}$), *Sterculia lychnophora* (1 g \cdot mL $^{-1}$), *Morus alba* (0.8 g \cdot mL $^{-1}$), *Citrus reticulata* (0.6 g \cdot mL $^{-1}$), *Euodia rutaecarpa* (0.3 g \cdot mL $^{-1}$) and *Trigonella foenum-graecum* (0.8 g \cdot mL $^{-1}$). The concentrations of all the indicated Chinese herbal medicine are as stated in the Pharmacopoeia of the People's Republic of China 2015. Samples (100 μ L) of the aqueous extract of *A. membranaceus* were mixed with methanol (900 μ L), and the mixture (50 μ L samples) was then analysed on a reverse-phase HPLC, and elution times of the mixture were compared with pure formononetin (Supporting Information Figure S2). We used a Dionex Summit HPLC on a 4.6 \times 250 mm Inertsil column with ODS-SP, 5.0 μ m from GL Sciences Inc (address). HPLC was carried out with a mobile phase: CH $_3$ CN and H $_2$ O (32: 68), at a flow rate of 1.0 mL \cdot min $^{-1}$ and using a detection wavelength of 254 nm.

Differentiated mature adipocytes were treated in DMEM plus 10% FBS with the addition of the vehicle or an indicated

Chinese herbal medicine water extract or indicated agents [A. membranaceus polysaccharide (MCE, Guangzhou, China), astragaloside IV (Sigma), formononetin (Selleck, Shanghai, China), calycosin (MCE) and StemRegenin 1 (SR1, Selleck)] for 24 h. After that, the cells were collected for real-time qPCR analysis.

RNA extraction and quantitative PCR

Total RNA was isolated with Trizol (Invitrogen), and first-strand cDNA was synthesized with Superscript III Reverse Transcriptase (Invitrogen, Shanghai, China) with 0.5 µg of RNA as the template for each reaction. The mRNA levels were quantified under optimized conditions with SYBR Premix Ex Taq (Takara Bio, Shanghai, China) following the manufacturer's instructions. The reference gene was 18S ribosomal RNA as an internal standard. The average mRNA levels of the genes were normalized to the control adipocytes or the adipose tissues in the control mice.

Mice

All animal care and experimental procedures were conducted in accordance with the Guide for the Care and Use of Laboratory Animals and were approved by the Animal Care and Use Committee of Guangzhou Institute of Biomedicine and Health, Chinese Academy of Sciences. Animal studies are reported in compliance with the ARRIVE guidelines (Kilkenny *et al.*, 2010; McGrath and Lilley, 2015). C57BL/6J mice fed a high-fat diet are routinely used as obesity mouse models (Bi *et al.*, 2014; Dominguez *et al.*, 2014).

Eight-week-old male C57BL/6J mice (Beijing Vital River Laboratory Animal Technology Co., Ltd., Beijing China) were maintained on a 12 h light/12 h dark cycle at 23°C in a specific pathogen-free environment. Mice were allowed access to different diets and water *ad libitum* and housed in groups of four in separate cages. The mice were fed on a high-fat diet (D12492, Research Diets, New Brunswick, NJ) for 8 weeks to become obese and then randomly divided into two groups and gavaged for the following 8 weeks with either formononetin (50 mg·kg⁻¹) or vehicle (control). All groups of mice continued on the high-fat diet. The high-fat diet provided 21.9 kJ·g⁻¹: 60% of energy from fat, 20% from protein and 20% from carbohydrate. Food intake and body weights were measured weekly. The rectal temperature was measured at 12 h after cold exposure (4°C). After feeding, the mice were killed by cervical dislocation. These results were analysed by an investigator, blinded to the treatment of the mice.

Histology

Brown interscapular, inguinal and epididymal adipose tissues were fixed in 4% formaldehyde overnight at room temperature, embedded in paraffin and cut into 5 µm sections with a microtome. The slides were deparaffinized, rehydrated and stained with haematoxylin and eosin (Sigma) following a standard protocol (Cardiff *et al.*, 2014). Sections were examined by light microscopy (Motic BA600, Beijing, China) and photographed with a Moticam Pro 285A. Photomicrographs were scanned with an Abaton Scan 300 colour scanner.

Indirect calorimetry and calculated energy expenditure

Whole-body oxygen consumption was measured with an open-circuit indirect calorimetry system with automatic temperature and light controls (Comprehensive Lab Animal Monitoring System, Columbus Instruments, OH). Mice had *ad libitum* access to chow and water in respiration chambers, and data were recorded for 48 h, including 24 h of acclimatization. Energy expenditure was calculated as recommended by the manufacturer.

Glucose tolerance test (GTT)

Mice were fasted overnight for 12 hours and then injected (i.p.) with 15% glucose solution (w/v) at a dose of 2 g kg⁻¹. Blood glucose was measured in tail vein blood with a glucometer (ACCU-CHEK Advantage, Roche Diagnostics, Guangzhou, China) at various time points after the injection of glucose.

Magnetic resonance imaging (MRI) analysis

This MRI analysis was carried out using the Minispec LF90 equipment (Bruker, Beijing, China). The mice were weighed and put into the sample holder without anaesthesia. The holder was then inserted into the machine for measurement, as described by Tinsley *et al.* (2004). The data in Figs 2C and 2D were obtained at 8 weeks.

PPAR γ luciferase activity assay

The PPAR γ luciferase activity assay was performed as described previously (Malapaka *et al.*, 2012). Briefly, COS-7 cells from ATCC (Beijing, China) were grown to 70% confluence in DMEM supplemented with 10% FBS and antibiotics. Then the COS-7 cells were transiently co-transfected with 100 ng of a plasmid containing the luciferase gene under the control of three tandem PPAR-response elements (PPAR-response element x 3 TK-luciferase) and 50 ng of full-length human PPAR γ plasmids using Lipofectamine 2000 (Invitrogen). After 24 h, the transfected cells were treated with DMSO, formononetin or rosiglitazone for an additional 24 h. Reporter luciferase assay kits from Promega (Guangzhou, China) were used to measure the luciferase activity following the manufacturer's instructions with a luminometer (Turner Biosystems, Sunnyvale, CA).

AlphaScreen binding assays

The ligand binding domain (LBD) of human PPAR γ (residues 206–477) containing a His6 tag was expressed as described previously (Li *et al.*, 2008). This assay uses the binding of the co-activator of PPAR γ , PGC-1 α -1 peptide to the LBD of PPAR γ which was determined by AlphaScreen assays using a hexahistidine detection kit from PerkinElmer Life Sciences (Guangzhou, China). The experiments were conducted with 20 nM His tag receptor LBD and 20 nM biotinylated PGC1 α -1 peptide in the presence of 5 µg·mL⁻¹ donor and acceptor beads in a buffer containing 50 mM MOPS, pH 7.4, 50 mM NaF, 50 mM CHAPS and 0.1 mg·mL⁻¹ bovine serum albumin. The biotinylated peptides of PGC-1 α -1 were AEEPSLLKLLAPA.

siRNA transfection

The siRNA oligonucleotides (Pparg, AUGACCUGAAGCUC CAAGAA; control, AGGGUGAACUCACGUCAGAA) were designed and synthesized by RiboBio Company (Guangzhou, China). On day 8 of differentiation, siRNA (20 nmol) was transfected into the primary adipocytes with Lipofectamine 2000 (Invitrogen) according to the manufacturer's instructions. Eight hours after transfection, the medium was replaced with a normal culture medium. The adipocytes were treated with the indicated agents for 48 h, or longer as indicated, and then harvested for analysis.

Analysis of oxygen consumption rate of adipocytes

The oxygen consumption rate (OCR) of the cells was analysed using the XFe24 Seahorse bioanalyzer (Agilent, Beijing, China). One day prior to the analysis, the cells were treated with formononetin (1 μM) or DMSO. After 24 h, the cells were equilibrated in sodium bicarbonate-free DMEM for 1 h in a CO₂-free incubator. After measuring the basal OCR, the following drugs (as final concentrations) were sequentially added to each well: oligomycin (5 μM), FCCP (5 μM) and rotenone (3 μM) + antimycin (5 μM); all compounds from Sigma.

Culture of 3T3-L1 cells and induction of differentiation

The 3T3-L1 pre-adipocytes were cultured in DMEM (Gibco) with 10% (v/v) FBS (Hyclone). Two days after the cells reached confluence (day 0), they were transferred to an MDI differentiation medium containing insulin (5 $\mu\text{g}\cdot\text{mL}^{-1}$), dexamethasone (1 μM), IBMX (0.5 mM) and either the vehicle, formononetin (1 μM) or rosiglitazone (1 μM). Two days later, the medium was replaced with DMEM supplemented with 10% FBS, insulin (5 $\mu\text{g}\cdot\text{mL}^{-1}$) plus and either the vehicle, formononetin (1 μM) or rosiglitazone (1 μM). The cells were subsequently re-fed every 2 days until day 6.

For Oil Red O staining, the 3T3-L1 adipocytes were fixed with 10% formalin for 5 min and then incubated in fresh formalin for 1 h. After washing with 60% (v/v) isopropanol in water, the cells were stained for 10 min in freshly diluted Oil Red O (2 mg·mL⁻¹ in 60% isopropanol). For quantitative analysis, Oil Red O was eluted from the cells by incubation with 100% isopropanol (400 μL per well) for 10 min, at room temperature, after which the optical density was determined at 500 nm with a spectrophotometer (Beckman Coulter). Oil Red O was prepared in 60% isopropanol for the standard curve.

Data and statistical analysis

The data and statistical analysis comply with the recommendations on experimental design and analysis in pharmacology (Curtis *et al.*, 2015). Data are expressed as means \pm SEM. ANOVA and unpaired, two-tailed *t*-tests were used for most comparisons in GraphPad Prism 5 (GraphPad, San Diego, CA, USA). *Post hoc* tests were run only when *F* achieved $P < 0.05$ and there was no significant variance in homogeneity. Tukey's HSD test was used for body weight gain and GTT data. To control for unwanted sources of variation, data were normalized to an internal standard (see Results for more details). $P < 0.05$ was considered significant.

Nomenclature of targets and ligands

Key protein targets and ligands in this article are hyperlinked to corresponding entries in <http://www.guidetopharmacology.org>, the common portal for data from the IUPHAR/BPS Guide to PHARMACOLOGY (Harding *et al.*, 2018), and are permanently archived in the Concise Guide to PHARMACOLOGY 2017/18 (Alexander *et al.*, 2017a,b,c).

Results

Formononetin derived from *A. membranaceus* induced adipocyte thermogenesis *in vitro*

Because brown and beige adipocytes use the same molecular mechanism in the regulation of *Ucp1* expression, primary inguinal adipocytes were used to screen several Chinese herbal medicine preparations for their effects on the expression of *Ucp1* in these cells. Isolated adipose stromal cells from the inguinal adipose tissue were differentiated into mature adipocytes *in vitro*, after which they were treated with the different Chinese herbal aqueous extracts for 24 h. The cells were then harvested for qPCR analysis. As shown in Figure 1 A, the *A. membranaceus* extract was the only preparation to enhance the expression of *Ucp1* in these adipocytes. This *A. membranaceus* extract is known to contain several different compounds, including *A. membranaceus* polysaccharide, astragaloside, formononetin and calycosin (Agyemang *et al.*, 2013). To identify the constituents of the *A. membranaceus* aqueous extract that were involved in the induction of *Ucp1* expression in adipocytes, each of these constituents was used to treat the adipocytes separately. The *A. membranaceus* polysaccharide is the largest component of the *A. membranaceus* aqueous extract but had no effect on *Ucp1* expression (Figure 1B). Astragaloside IV, which has been reported to regulate adiponectin secretion in adipocytes (Xu *et al.*, 2009), had no effect on adipocyte *Ucp1* either (Figure 1C). However, formononetin, an O-methylated isoflavone (Figure 1D), but not its analogue calycosin (Figure 1E and Supporting Information Figure S1), did increase the expression of *Ucp1*, dose-dependently. Furthermore, treatment with a combination of the *A. membranaceus* aqueous extract (2 mg·mL⁻¹) and formononetin (1 μM) showed no additive or inhibitory effects on the expression of *Ucp1*. Additionally, formononetin (1 μM) elevated the expression of other relevant genes for PRDM16, PGC-1 α , Type II iodothyronine deiodinase (Dio2), and the cell death activator (Cidea) protein (Figure 1G). HPLC analysis demonstrated that there was a significant amount of formononetin (28.6 \pm 1.2 $\mu\text{g}\cdot\text{mL}^{-1}$, 107 μM) in the 2 mg·mL⁻¹ aqueous extract of *A. membranaceus* (Supporting Information Figure S2). Thus, formononetin appears to be the only known constituent that could account for the effect of *A. membranaceus* extracts on *Ucp1* expression in adipocytes. Immunofluorescent staining showed that formononetin (1 μM) also increased the UCP1 protein level (Figure 1H). The effect of formononetin on adipocytes was further assessed using the Seahorse bioanalyzer, which indicated that treatment of the cells with formononetin (1 μM) increased both basal and uncoupled mitochondrial respiration (Figure 1I).

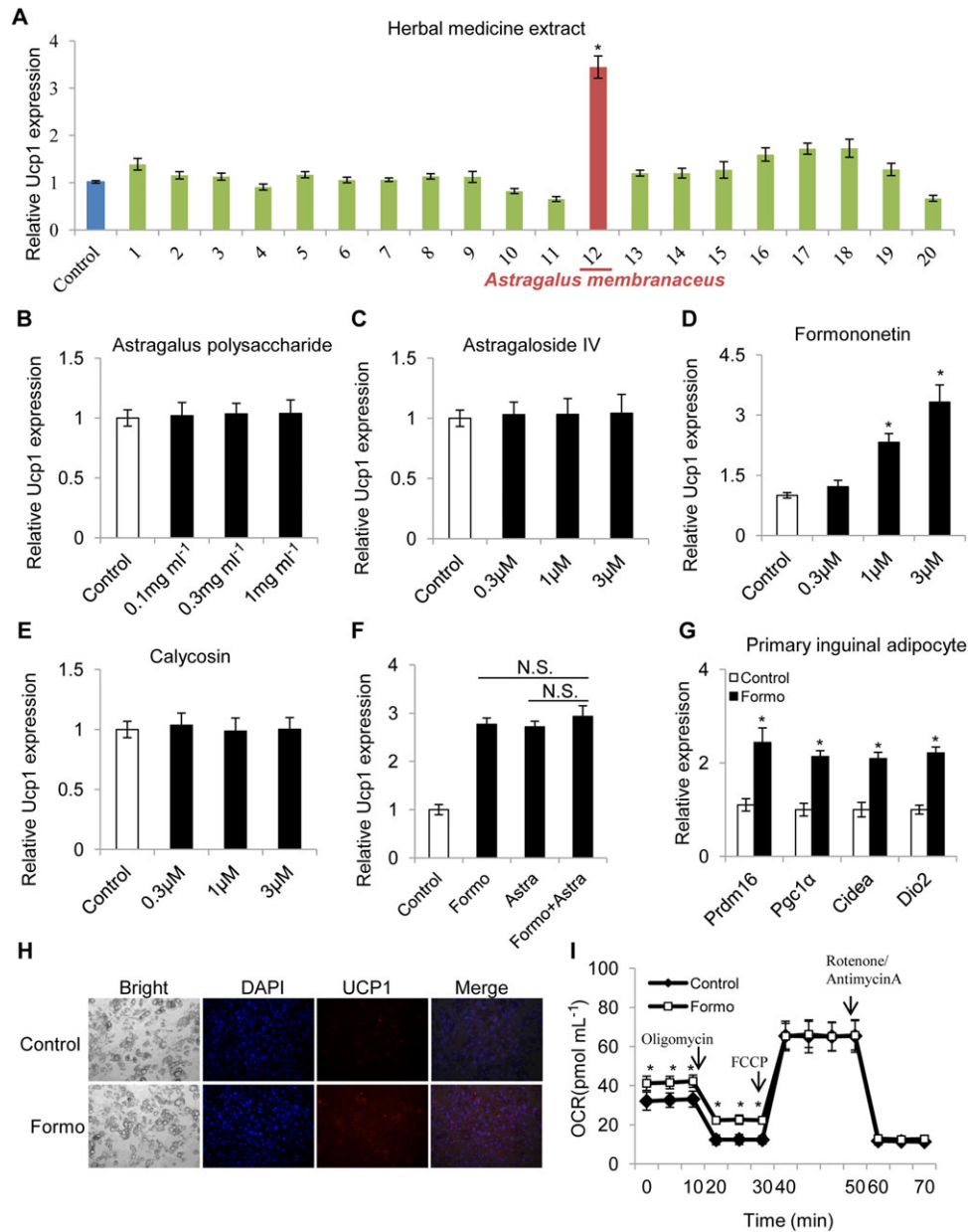


Figure 1

Effects of Chinese herbal medicine extracts and some constituents of extracts of *A. membranaceus* on expression of *Ucp1* in adipocytes *in vitro*. Inguinal adipose stromal cells were differentiated into adipocytes and then treated with different Chinese herbal medicine extracts at a ratio of 1:1000 for 24 h and harvested for qPCR. (A) *Ucp1* mRNA expression in primary inguinal adipocytes after treatment with various Chinese herbal medicine extracts ($n = 5$): 1. *Cichorium intybus* (1.5 mg·mL⁻¹); 2. *Cinnamomum cassia* (0.3 mg·mL⁻¹); 3. *Coix lachryma-jobi* (1.0 mg·mL⁻¹); 4. *Zingiber officinale* (1 mg·mL⁻¹); 5. *Eucommia ulmoides* (1.2 mg·mL⁻¹); 6. *Eugennia caryophyllata* (0.2 mg·mL⁻¹); 7. *Sophora japonica* (0.8 mg·mL⁻¹); 8. *Hippophae rhamnoides* (0.42 mg·mL⁻¹); 9. *Alpinia officinarum* (0.5 mg·mL⁻¹); 10. *Lonicera japonica* (1 mg·mL⁻¹); 11. *Morus alba* (1.2 mg·mL⁻¹); 12. *A. membranaceus* (2 mg·mL⁻¹); 13. *Atractylodes lancea* (0.6 g·mL⁻¹); 14. *Lycium barbarum* (1.2 mg·mL⁻¹); 15. *Piper nigrum* (0.1 mg·mL⁻¹); 16. *Sterculia lychnophora* (1 mg·mL⁻¹); 17. *Morus alba* (0.8 mg·mL⁻¹); 18. *Citrus reticulata* (0.6 mg·mL⁻¹); 19. *Euodia rutaecarpa* (0.3 mg·mL⁻¹); and 20. *Trigonella foenum-graecum* (0.8 mg·mL⁻¹). (B–E) Effects of some constituents of the aqueous extract of *A. membranaceus* on *Ucp1* expression in primary differentiated inguinal adipocytes were analysed by qPCR. (B) astragalus polysaccharide, (C) astragaloside IV, (D) formononetin and (E) calycosin ($n = 5$ for each). (F) Effects of the combination of *A. membranaceus* extract and formononetin on *Ucp1* expression ($n = 5$). (G) Expression of genes involved in thermogenesis (for PRDM16, PGC1 α , CIDEA, Dio2) in primary inguinal adipocytes ($n = 5$) after treatment with formononetin (1 μ M). For quantitative RT-PCR experiments, 18S ribosomal RNA was adopted as an internal standard to control for unwanted sources of variation. The average mRNA levels of thermogenic genes were normalized to the blank control (baseline). (H) Immunofluorescent staining of adipocytes treated with DMSO (control) or formononetin (1 μ M). (I) Oxygen consumption rate (OCR) in primary inguinal adipocytes treated with DMSO (control) or formononetin (1 μ M); $n = 5$ well per group. Data represent mean \pm SEM from 5 independent experiments, each carried out with triplicate samples. * $P < 0.05$, significantly different from control.

Decreased diet-induced obesity in mice treated with formononetin

Given that other constituents in the aqueous extract of *A. membranaceus* may also influence body weight in obese mice, diet-induced obese (DIO) mice were treated with only formononetin (50 mg kg⁻¹ daily) for 8 weeks. Bodyweight and food intake were measured weekly. After 6 weeks of treatment, the formononetin-treated mice showed lower bodyweight than the control mice (Figure 2A) but the food intake did not differ between these two groups of mice (Figure 2B). Analysis by whole body MRI suggested that treatment with formononetin for 8 weeks reduced only fat mass but not lean mass in DIO mice (Figure 2C). Consistent with this finding, the inguinal and epididymal adipose tissue weights were lower in treated mice than in the controls (Figure 2D). Haematoxylin and eosin staining analysis also confirmed that the size of the adipocytes in the adipose tissue was smaller in formononetin-treated mice than in the control mice (Figure 2E, F). Consistent with these findings, insulin sensitivity, as measured by the GTT, was improved in the formononetin treated mice (Figure 2G).

As expected, expression of the thermogenic genes was increased in the inguinal, epididymal and brown adipose tissues (BAT) of formononetin-treated mice (Figure 2H–J). UCP1 protein expression in both the brown and inguinal adipose tissue of the formononetin-treated mice was enhanced in the Western blot analysis (Figure 2K and Supporting Information Figure S3). Indirect calorimetry analysis proved that O₂ consumption, body temperature, CO₂ production and energy expenditure were higher in mice treated with formononetin while no difference in locomotor activity was observed (Figure 2L–N and Supporting Information Figure S4). To further delineate the molecular mechanism(s) underlying the effects of formononetin in DIO mice, these mice were placed in a thermoneutral environment (30°C) where mice no longer need to activate adipocyte thermogenesis to maintain body temperature. The mice were then treated with vehicle or formononetin for 8 weeks, as before. Under conditions of thermoneutrality, there were no significant differences in body weight between the two groups (Supporting Information Figure S5). Taken together, our results showed that formononetin, a constituent of the aqueous extract of *A. membranaceus*, can reduce bodyweight gain in obese mice by increasing adipocyte thermogenesis.

PPAR γ mediates the effects of formononetin

Several studies have reported that formononetin is a potential ligand of oestrogen receptors (ERs), aryl hydrocarbon receptors (AhRs) and PPAR α/γ (Medjakovic and Jungbauer, 2008). ERs are unlikely to be the targets of formononetin in terms of adipocyte thermogenesis, as oestrogen has been reported to have no effect on *Ucp1* induction in brown adipocytes, and the ER antagonist tamoxifen can induce thermogenesis *in vivo* (Andersen *et al.*, 2014; Hesselbarth *et al.*, 2015). In addition, we tested the effects of a known AhR antagonist, StemRegenin1, and found it had no effect on *Ucp1* expression induced by formononetin (Supporting Information Figure S6). To test the effects of combining formononetin with the other known agonists, differentiated adipocytes were treated with 1 μ M formononetin together

with 1 μ M AM580 (RAR agonist), 1 μ M bexarotene (RXR agonist), 1 μ M CL316243 (β_3 -adrenoceptor agonist), 1 μ g mL⁻¹ FGF21 or 1 μ M WY14643 (PPAR α agonist), and these compounds alone for 24 h. As shown in Figure 3A and B, the effects of combining formononetin with these other known thermogenesis inducers, showed a more than additive effect on *Ucp1* expression with all other inducers, except for rosiglitazone. The aqueous extract of *A. membranaceus* (2 mg mL⁻¹) had no additive effect with rosiglitazone on adipocyte thermogenesis either (Figure 3C). These results suggest that formononetin has the same molecular target as rosiglitazone. Thus, the PPAR γ plasmid and PPAR response element (PPRE)-luciferase reporter were used to carry out a PPAR γ activation assay, and as expected, both formononetin (Figure 3D) and rosiglitazone dose-dependently promoted luciferase activity (Supporting Information Figure S7). Furthermore, siRNA knockdown of *Ppar γ* blocked the increased *Ucp1* expression induced by formononetin (Figure 3E and Supporting Information Figure S8). To demonstrate that formononetin can bind directly with PPAR γ , we used an AlphaScreen binding assay (Li *et al.*, 2008). In this assay, the co-activator peptide PGC-1 α and the PPAR γ LBD protein were attached to donor and acceptor beads respectively. Upon interaction between the co-activator peptide PGC-1 α and the PPAR γ LBD, excitation with a laser beam at 680 nm causes the donor beads to emit single oxygen molecules that activate fluorophores in the acceptor beads, and the light is recorded at 520–620 nm. The known ligand for the PPAR γ LBD, rosiglitazone, induced a strong interaction, and the results clearly demonstrated that formononetin can also bind directly with the ligand-binding domain of PPAR γ (Figure 3F). However, its PPAR γ activity was only about 10% that of rosiglitazone. Rosiglitazone is a thiazolidinedione developed for the treatment of diabetes, but it induced obesity in mice, whereas our results showed that formononetin treatment inhibits the development of weight gain (obesity). Obesity is accompanied by adipogenesis, and as *Ppar γ* is the master gene for adipogenesis; we compared the roles of the two compounds in adipogenesis. As shown in Figure 3G and H, formononetin (1 μ M) promoted only mild adipogenesis in 3T2-L1 cells, compared with rosiglitazone (1 μ M) under the MDI cocktail and, unlike rosiglitazone, it could not induce adipocyte formation in the presence of insulin (5 μ g mL⁻¹) alone. Thus, the limited ability of formononetin to stimulate adipogenesis is likely to account for the reduced bodyweight gain, compared to the weight gain after rosiglitazone (30 mg⁻¹ kg⁻¹ day⁻¹ for 2 weeks) in C57BL/6J mice (Sell *et al.*, 2004). Based on these results, we summarized our findings in a diagram to illustrate the mechanisms underlying thermogenesis induced by formononetin and extracts of *A. membranaceus* (Figure 4).

Discussion

The thiazolidinedione compounds (“glitazones”) developed as ligands for PPAR γ were widely used to treat diabetes and promote insulin sensitivity, but their side effects, including increased body weight and liver fat, have restricted their use (Ahmadian *et al.*, 2013). It is therefore necessary to find a new PPAR γ -specific ligand that avoids these side effects while

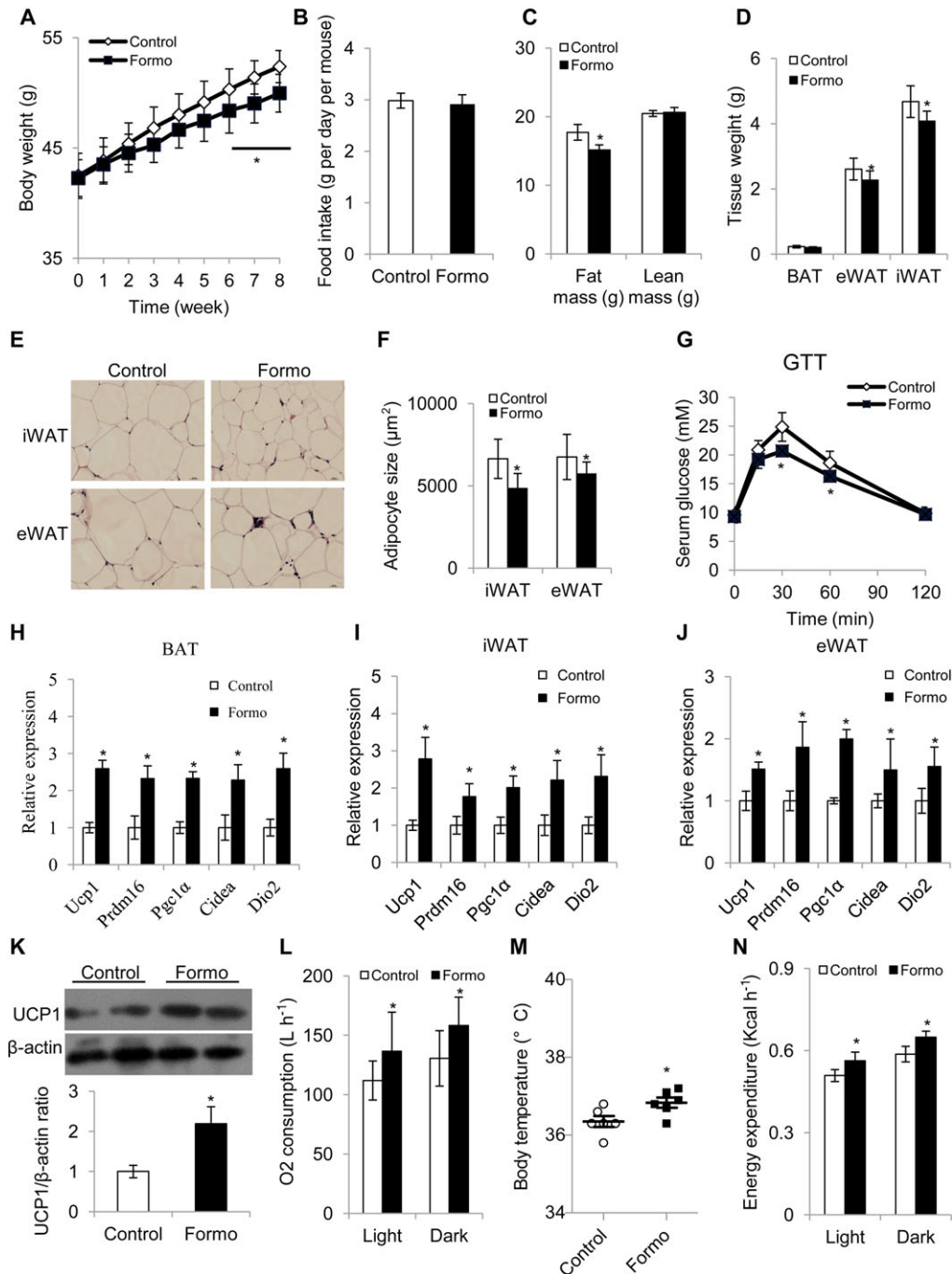


Figure 2

Treatment with formononetin (50 mg kg^{-1} ; once daily by gavage) for 8 weeks inhibited weight gain in mice with diet-induced obesity. (A–D) Eight-week-old C57BL/6J male mice ($n = 10$ mice) were fed a high-fat diet for 8 weeks to become obese and then treated with the vehicle (control) or formononetin for 8 weeks, continuing on the high-fat diet. Measurement of (A) food intake, (B) bodyweight, (C) body composition and (D) tissue weight. (E–F) Representative haematoxylin and eosin staining of epididymal WAT (eWAT) and inguinal WAT (iWAT); samples were taken at 8 weeks. (G) Glucose tolerance test ($n = 10$ mice). (H–J) Quantitative PCR analysis of thermogenic genes in (H) iWAT, (I) eWAT and (J) BAT from mice treated with the vehicle (control) or with formononetin for 8 weeks ($n = 5$ per group). For quantitative RT-PCR experiments, 18S ribosomal RNA was adopted as an internal standard to control for unwanted sources of variation. The average mRNA levels of thermogenic genes were normalized to the control mice (baseline). (K) Western blot analysis of UCP1 in BAT (above) and densitometric analysis of the relative abundance of UCP1 (below) ($n = 5$), β -actin was adopted as an internal standard to control for unwanted sources of variation, and the ratio of UCP-1 expression in BAT was normalized to that in control mice (baseline). (L) Oxygen consumption ($n = 5$). (M) Body temperature ($n = 5$). (N) Energy expenditure ($n = 5$). Vehicle was used as control. Data represent mean \pm SEM from 5 independent experiments, each carried out with triplicate samples. * $P < 0.05$, significantly different from control.

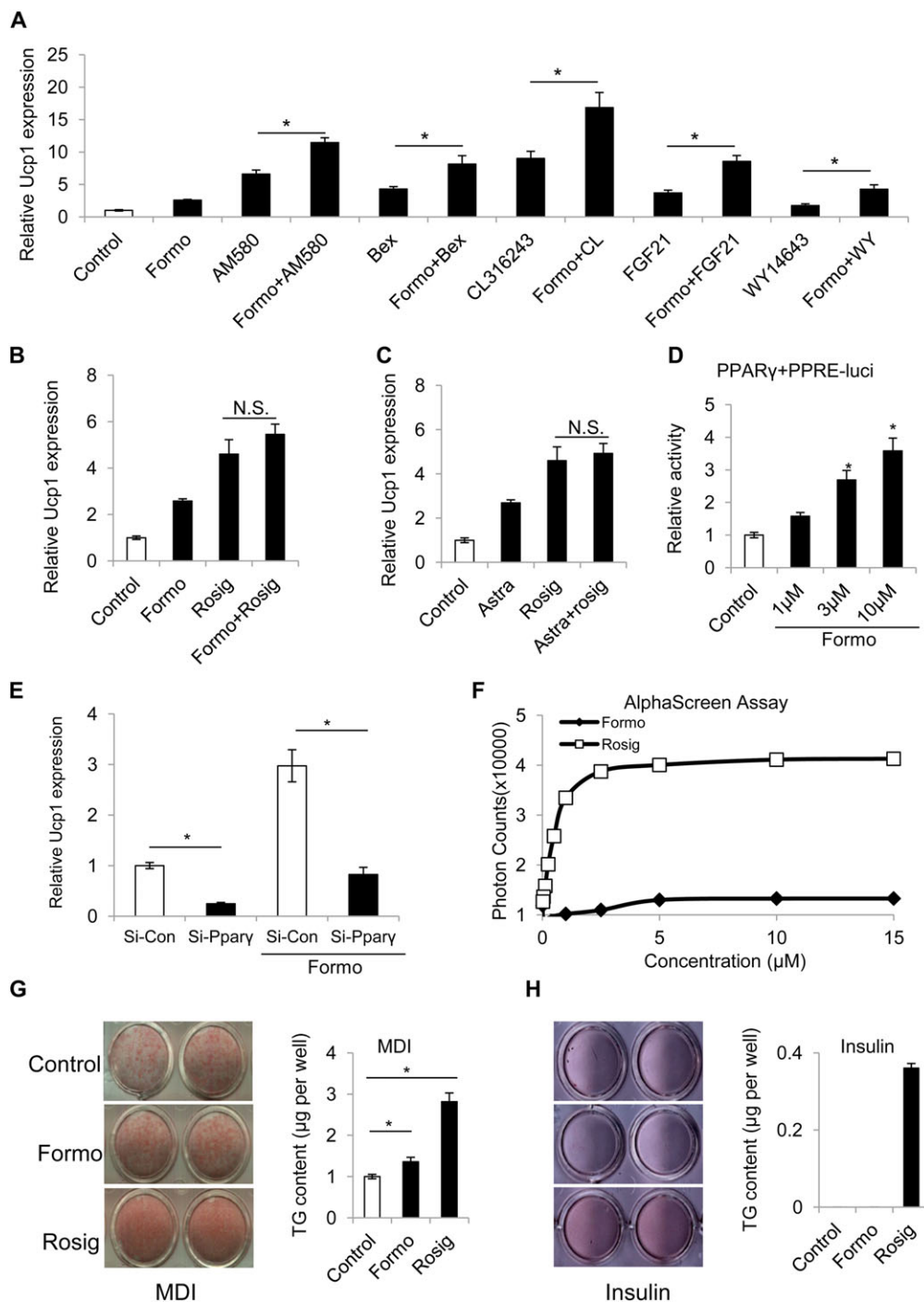


Figure 3

The effects of formononetin are mediated by PPAR γ . (A) Effects of combining formononetin (1 μ M) with different known thermogenic agents, on *Ucp1* expression in differentiated inguinal adipocytes. (B) Combination of formononetin and rosiglitazone. (C) formononetin and *A. membranaceus* extract ($n = 5$). For quantitative RT-PCR experiments, 18S ribosomal RNA was adopted as an internal standard to control for unwanted sources of variation. The average mRNA expression of *Ucp1* was normalized to the blank control (baseline). (D) Formononetin dose-dependently promoted luciferase activity in COS7 cells transfected with PPAR γ and PPRE-luciferase plasmids ($n = 5$). The luciferase activity was normalized to the blank control (baseline). (E) siRNA knockdown of *Ppar γ* impaired induction of *Ucp1* by formononetin ($n = 5$). 18S ribosomal RNA was adopted as an internal standard to control for unwanted sources of variation. The average mRNA expression of *Ucp1* was normalized to the si-RNA control as baseline. (F) Dose-dependent increase of the binding of PGC-1 α -1 to the PPAR γ LBD, induced by rosiglitazone or formononetin, using the AlphaScreen assay ($n = 5$). (G, H) Oil Red O staining (left) and quantitation of TG contents (right) of 3T3-L1 differentiated cells with the vehicle (control), rosiglitazone or formononetin under (G) MDI cocktail and (H) insulin only ($n = 5$). Data represent mean \pm SEM from 5 independent experiments, each carried out with triplicate samples. * $P < 0.05$, significantly different as indicated.

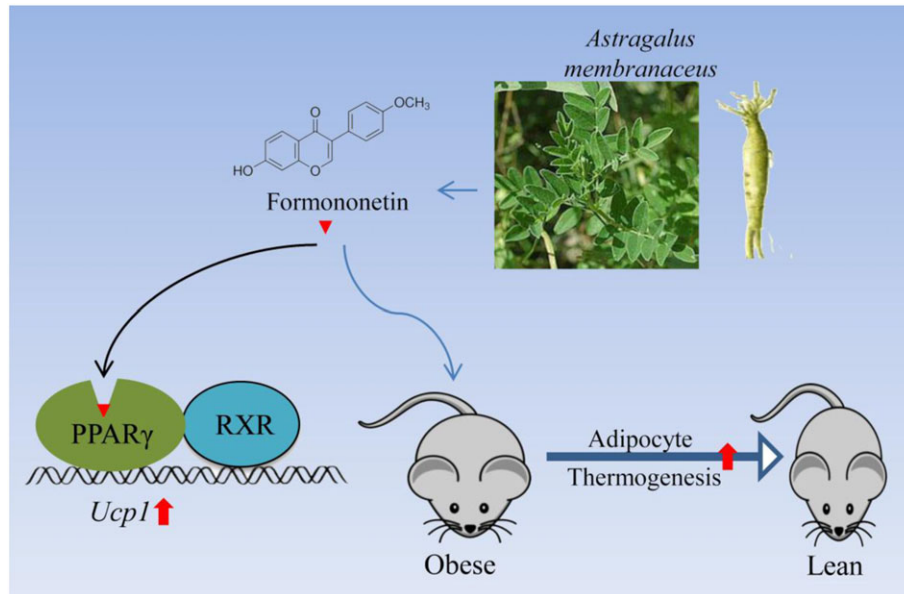


Figure 4

Schematic diagram of the mechanism(s) underlying the induction of adipocyte thermogenesis, by formononetin and the aqueous extract of *A. membranaceus*. This extract and one of its components, formononetin, block the development of obesity induced by high-fat diets, by promoting adipocyte thermogenesis. Formononetin binds with PPAR γ to form a heterodimer with RXR to drive expression of *Ucp1* in adipocytes.

retaining the insulin-sensitizing effect. PPAR γ is the master regulatory gene for adipocyte formation, and Ppar γ knockout mice died *in utero* (Gregoire *et al.*, 1998). Rosiglitazone is a classical agonist of PPAR γ and widely used as an inducer of adipogenesis, as it easily leads to body weight increase in mice. Recently, SR1664 was identified as a new non-classical agonist of PPAR γ , i.e., that exhibited only some of the effects of the classical agonist rosiglitazone. Thus, SR1664 had no effect on adipogenesis but still exerted an anti-diabetic effect on obese mice, without many other unwanted side effects typical of the classical agonist (Choi *et al.*, 2011). **Telmisartan**, an angiotensin AT $_1$ receptor antagonist, marketed for the treatment of hypertension, has also been shown to be a non-classical agonist of PPAR γ , but it decreases body weight gain, unlike rosiglitazone (Araki *et al.*, 2006). In addition, other experimental compounds that are non-classical agonists of PPAR γ , such as **nTzDpa**, KR-62980 and halofenate (Zhang *et al.*, 2007), not only have limited adipogenic ability *in vitro* but also inhibit body weight increase *in vivo*. Interestingly, these poorly known agonists showed little effect on thermogenesis (Ohno *et al.*, 2012). In the present study, we found that the natural product formononetin is also a weak, non-classical agonist of PPAR γ but this compound increased expression of *Ucp1* and thermogenesis, both *in vivo* and *in vitro*. Another non-classical agonist of PPAR γ , calycosin, which has a structure analogous to formononetin, showed no effect on the expression of *Ucp1*. Consistent with the earlier studies, as a non-classical agonist, formononetin had poor adipogenic capacity and did not lead to increased body weight increase. In addition, liver weight and TG content in mice treated with formononetin showed no significant differences from that of control mice, excluding the fatty liver side effect of rosiglitazone (Supporting Information Figure S9). It

is noteworthy that classical agonists of PPAR γ , such as rosiglitazone, increase the protein expression of UCP1 in adipocytes both *in vitro* and *in vivo* but have no effect on energy expenditure *in vivo* (Sell *et al.*, 2004). Sell *et al.* studied 2-(2-[4-phenoxy-2-propylphenoxy]ethyl)indole-5-acetic acid, a classical PPAR γ agonist with similar structure to rosiglitazone, and reported that this compound strongly increased protein levels of UCP1 in both BAT and WAT in wild-type C57BL/6J and *ob/ob* obese mice, without enhancing energy expenditure. In contrast, we found formononetin clearly up-regulated UCP1 protein and increased energy expenditure, while a similarly non-classical PPAR γ agonist, calycosin, did neither. Therefore, different PPAR γ ligands can induce different responses (Hughes *et al.*, 2012). Although the detailed molecular mechanism was not clear, it is possible that expression of additional genes and/or different levels of the induced genes by modulation of PPAR γ activity play critical roles in the functional thermogenesis mediated by activated UCP1 protein. Indeed, Fmoc-L-Leu, a weak non-classical PPAR γ agonist, which is about 100 to 1000-fold less potent than rosiglitazone, has a capacity to induce UCP1 expression and to decrease adipogenic potential, similar to that of formononetin (Rocchi *et al.*, 2001; Mao *et al.*, 2017). In our experiments, it is unlikely that formononetin affected the β_3 -adrenoceptor signalling pathway, because of the following results. First of all, the effects of formononetin were additive to those of the β_3 -adrenoceptor agonist CL316243 (Figure 3A). Secondly, formononetin increased expression of UCP1 but did not reduce weight gain in mice under thermoneutral conditions (Supporting Information Figure S5), suggesting sympathetic activation is essential for its activity. However, more clinical experiments are clearly needed to determine if formononetin is a suitable compound for the treatment

of obesity and diabetes in patients. Nonetheless, our study has suggested a possible direction to explore and that formononetin might serve as a potential drug candidate of a non-classical agonist for PPAR γ , based on its beneficial effects on obesity and insulin resistance.

Extracts of *A. membranaceus* are a traditional Chinese herbal medicine that has been widely used with almost no harm to human health and, more importantly, it is commonly used in China, as a daily herbal supplement to maintain health. For example, it is used to make soup with chicken, Chinese dates (*Ormosia hosiei*) or other foods (Song *et al.*, 2014). To elucidate the possible molecular mechanisms underlying the effects of such extracts, some of its many constituents, which include polysaccharides, saponins and flavonoids, have been isolated and their actions analysed. Among these, the astragalus polysaccharides have been most studied and found to be beneficial for insulin resistance and cardiac hypertrophy (Liu *et al.*, 2014; Luan *et al.*, 2015). Astragaloside IV (a saponin) has been reported to regulate adiponectin secretion and improve insulin resistance in obese mice (Xu *et al.*, 2009). However, the roles of the other constituents remain poorly characterized. In this report, a new action of the extract of *A. membranaceus* and of one of its constituents, formononetin, to stimulate adipocyte thermogenesis by modulating PPAR γ activity has been described. Our results are compatible with the belief that extracts of *A. membranaceus* and one of its constituent, formononetin, support health and reduce obesity.

Acknowledgements

This study was supported in part by the National Basic Research Program of China (2016YFC1305000 and 2010CB945500), the strategic priority program on development of new drug of the Chinese Academy of Sciences (XDA12040325), Natural Science Foundation of China (81700742, 81400825, 81774134, 81327801 and 31301019), a key international collaborative fund from the Chinese Academy of Sciences (154144KYSB20150019), Natural Science Foundation of Guangdong province (2016A030310122), International collaborative funds from Guangdong Province (2013B051000090 and 2015A050502041), Science and Technology Planning Project of Guangdong Province (2017B030314056) and Guangdong Provincial Public interest research and capacity building projects (2014A010107024).

Author contributions

T.N., S.Z., L.M., Y.Y., W.S., X.L., S.L., K.L. and Y.S. performed the experiments. T.N., Z.Z., A.X., C.W.M., P. L., S.L., Y.X., C.W., P. D. and D.W. analysed and interpreted the data. T.N. and D.W. conceived and designed the experiments. T.N., X.H. and D.W. wrote and edited the manuscript. D.W. is the guarantor of this work and, as such, has full access to all the data in the study and takes responsibility for the integrity of the data and the accuracy of the data analysis.

Conflict of interest

The authors declare no conflicts of interest.

Declaration of transparency and scientific rigour

This Declaration acknowledges that this paper adheres to the principles for transparent reporting and scientific rigour of preclinical research recommended by funding agencies, publishers and other organisations engaged with supporting research.

References

- Agyemang K, Han L, Liu E, Zhang Y, Wang T, Gao X (2013). Recent advances in *Astragalus membranaceus* anti-diabetic research: pharmacological effects of its phytochemical constituents. *Evid Based Complement Alternat Med* 2013 654643.
- Ahmadian M, Suh JM, Hah N, Liddle C, Atkins AR, Downes M *et al.* (2013). PPAR γ signaling and metabolism: the good, the bad and the future. *Nat Med* 19: 557–566.
- Alexander SPH, Kelly E, Marrion NV, Peters JA, Faccenda E, Harding SD *et al.* (2017a). The Concise Guide to PHARMACOLOGY 2017/18: Other proteins. *Br J Pharmacol* 174: S1–S16.
- Alexander SPH, Cidlowski JA, Kelly E, Marrion NV, Peters JA, Faccenda E *et al.* (2017b). The Concise Guide to PHARMACOLOGY 2017/18: Nuclear hormone receptors. *Br J Pharmacol* 174: S208–S224.
- Alexander SPH, Christopoulos A, Davenport AP, Kelly E, Marrion NV, Peters JA *et al.* (2017c). The Concise Guide to PHARMACOLOGY 2017/18: G protein-coupled receptors. *Br J Pharmacol* 174: S17–S129.
- Andersen C, Kotowska D, Tortzen CG, Kristiansen K, Nielsen J, Petersen RK (2014). 2-(2-Bromophenyl)-formononetin and 2-heptyl-formononetin are PPAR γ partial agonists and reduce lipid accumulation in 3T3-L1 adipocytes. *Bioorg Med Chem* 22: 6105–6111.
- Araki K, Masaki T, Katsuragi I, Tanaka K, Kakuma T, Yoshimatsu H (2006). Telmisartan prevents obesity and increases the expression of uncoupling protein 1 in diet-induced obese mice. *Hypertension* 48: 51–57.
- Bartel A, Heeren J (2014). Adipose tissue browning and metabolic health. *Nat Rev Endocrinol* 10: 24–36.
- Baskaran P, Krishnan V, Ren J, Thyagarajan B (2016). Capsaicin induces browning of white adipose tissue and counters obesity by activating TRPV1 channel-dependent mechanisms. *Br J Pharmacol* 173: 2369–2389.
- Bi P, Shan T, Liu W, Yue F, Yang X, Liang XR *et al.* (2014). Inhibition of Notch signaling promotes browning of white adipose tissue and ameliorates obesity. *Nat Med* 20 (8): 911–918.
- Buermann B, Toubro S, Astrup A (2000). Effects of the two beta3-agonists, ZD7114 and ZD2079 on 24 hour energy expenditure and respiratory quotient in obese subjects. *Int J Obes Relat Metab Disord* 24: 1553–1560.

- Cardiff RD, Miller CH, Munn RJ (2014). Manual hematoxylin and eosin staining of mouse tissue sections. *Cold Spring Harb Protoc* 2014: 655–658.
- Choi JH, Banks AS, Kamenecka TM, Busby SA, Chalmers MJ, Kumar N *et al.* (2011). Antidiabetic actions of a non-agonist PPAR γ ligand blocking Cdk5-mediated phosphorylation. *Nature* 477: 477–481.
- Cohen P, Levy JD, Zhang Y, Frontini A, Kolodin DP, Svensson KJ *et al.* (2014). Ablation of PRDM16 and beige adipose causes metabolic dysfunction and a subcutaneous to visceral fat switch. *Cell* 156: 304–316.
- Curtis MJ, Bond RA, Spina D, Ahluwalia A, Alexander SP, Giembycz MA *et al.* (2015). Experimental design and analysis and their reporting: new guidance for publication in BJP. *Br J Pharmacol* 172: 3461–3471.
- Cypess AM, White AP, Vernochet C, Schulz TJ, Xue R, Sass CA *et al.* (2013). Anatomical localization, gene expression profiling and functional characterization of adult human neck brown fat. *Nat Med* 19: 635–639.
- Di Cesare M, Bentham J, Stevens GA, Zhou B, Danaei G, Lu Y *et al.* (2016). Trends in adult body-mass index in 200 countries from 1975 to 2014: a pooled analysis of 1698 population-based measurement studies with 19.2 million participants. *Lancet* 387: 1377–1396.
- Dominguez E, Galmozzi A, Chang JW, Hsu KL, Pawlak J, Li W *et al.* (2014). Integrated phenotypic and activity-based profiling links Cc1 to obesity and diabetes. *Nat Chem Biol* 10: 113–121.
- Feldmann HM, Golozoubova V, Cannon B, Nedergaard J (2009). UCP1 ablation induces obesity and abolishes diet-induced thermogenesis in mice exempt from thermal stress by living at thermoneutrality. *Cell Metab* 9: 203–209.
- Fisher FM, Kleiner S, Douris N, Fox EC, Mepani RJ, Verdeguer F *et al.* (2012). FGF21 regulates PGC-1 α and browning of white adipose tissues in adaptive thermogenesis. *Genes Dev* 26: 271–281.
- Gregoire FM, Smas CM, Sul HS (1998). Understanding adipocyte differentiation. *Physiol Rev* 78: 783–809.
- Harding SD, Sharman JL, Faccenda E, Southan C, Pawson AJ, Ireland S *et al.* (2018). The IUPHAR/BPS Guide to PHARMACOLOGY in 2018: updates and expansion to encompass the new guide to IMMUNOPHARMACOLOGY. *Nucl Acids Res* 46: D1091–D1106.
- Hesselbarth N, Pettinelli C, Gericke M, Berger C, Kunath A, Stumvoll M *et al.* (2015). Tamoxifen affects glucose and lipid metabolism parameters, causes browning of subcutaneous adipose tissue and transient body composition changes in C57BL/6NTac mice. *Biochem Biophys Res Commun* 464: 724–729.
- Hughes TS, Chalmers MJ, Novick S, Kuruvilla DS, Chang MR, Kamenecka TM *et al.* (2012). Ligand and receptor dynamics contribute to the mechanism of graded PPAR γ agonism. *Structure* 20: 139–150.
- Kilkenny C, Browne W, Cuthill IC, Emerson M, Altman DG (2010). Animal research: reporting *in vivo* experiments: the ARRIVE guidelines. *Br J Pharmacol* 160: 1577–1579.
- Li Y, Kovach A, Suino-Powell K, Martynowski D, Xu HE (2008). Structural and biochemical basis for the binding selectivity of PPAR γ to PGC-1 α . *J Biol Chem* 283: 19132–19139.
- Liu H, Bai J, Weng X, Wang T, Li M (2014). Amelioration of insulin resistance in rat cells by Astragalus polysaccharides and associated mechanisms. *Exp Ther Med* 7: 1599–1604.
- Luan A, Tang F, Yang Y, Lu M, Wang H, Zhang Y (2015). Astragalus polysaccharide attenuates isoproterenol-induced cardiac hypertrophy by regulating TNF- α /PGC-1 α signaling mediated energy biosynthesis. *Environ Toxicol Pharmacol* 39: 1081–1090.
- Malapaka RR, Khoo S, Zhang J, Choi JH, Zhou XE, Xu Y *et al.* (2012). Identification and mechanism of 10-carbon fatty acid as modulating ligand of peroxisome proliferator-activated receptors. *J Biol Chem* 287: 183–195.
- Mao L, Nie B, Nie T, Hui X, Gao X, Lin X *et al.* (2017). Visualization and quantification of browning using a Ucp1-2A-luciferase knock-in mouse model. *Diabetes* 66: 407–417.
- McGrath JC, Lilley E (2015). Implementing guidelines on reporting research using animals (ARRIVE etc.): new requirements for publication in BJP. *Br J Pharmacol* 172: 3189–3193.
- Medjakovic S, Jungbauer A (2008). Red clover isoflavones biochanin A and formononetin are potent ligands of the human aryl hydrocarbon receptor. *J Steroid Biochem Mol Biol* 108: 171–177.
- Ohno H, Shinoda K, Spiegelman BM, Kajimura S (2012). PPAR γ agonists induce a white-to-brown fat conversion through stabilization of PRDM16 protein. *Cell Metab* 15: 395–404.
- Petrovic N, Walden TB, Shabalina IG, Timmons JA, Cannon B, Nedergaard J (2010). Chronic peroxisome proliferator-activated receptor γ (PPAR γ) activation of epididymally derived white adipocyte cultures reveals a population of thermogenically competent, UCP1-containing adipocytes molecularly distinct from classic brown adipocytes. *J Biol Chem* 285: 7153–7164.
- Rocchi S, Picard F, Vamecq J, Gelman L, Potier N, Zeyer D *et al.* (2001). A unique PPAR γ ligand with potent insulin-sensitizing yet weak adipogenic activity. *Mol Cell* 8: 737–747.
- Seale P, Bjork B, Yang W, Kajimura S, Chin S, Kuang S *et al.* (2008). PRDM16 controls a brown fat/skeletal muscle switch. *Nature* 454: 961–967.
- Sell H, Berger JP, Samson P, Castriota G, Lalonde J, Deshaies Y *et al.* (2004). Peroxisome proliferator-activated receptor γ agonism increases the capacity for sympathetically mediated thermogenesis in lean and ob/ob mice. *Endocrinology* 145: 3925–3934.
- Shabalina IG, Petrovic N, de Jong JM, Kalinovich AV, Cannon B, Nedergaard J (2013). UCP1 in brite/beige adipose tissue mitochondria is functionally thermogenic. *Cell Rep* 5: 1196–1203.
- Song QH, Xu RM, Zhang QH, Shen GQ, Ma M, Zhao XP *et al.* (2014). Combined effects of astragalus soup and persistent Taiji boxing on improving the immunity of elderly women. *Int J Clin Exp Med* 7: 1873–1877.
- Tinsley FC, Taicher GZ, Heiman ML (2004). Evaluation of a quantitative magnetic resonance method for mouse whole body composition analysis. *Obes Res* 12: 150–160.
- Villarroya F, Iglesias R, Giralt M (2007). PPARs in the control of uncoupling proteins gene expression. *PPAR Res* 2007: 74364.
- Wang S, Liang X, Yang Q, Fu X, Rogers CJ, Zhu M *et al.* (2015). Resveratrol induces brown-like adipocyte formation in white fat through activation of AMP-activated protein kinase (AMPK) α 1. *Int J Obes (Lond)* 39: 967–976.
- Xu A, Wang H, Hoo RL, Sweeney G, Vanhoutte PM, Wang Y *et al.* (2009). Selective elevation of adiponectin production by the natural compounds derived from a medicinal herb alleviates insulin resistance and glucose intolerance in obese mice. *Endocrinology* 150: 625–633.
- Zhang F, Lavan BE, Gregoire FM (2007). Selective modulators of PPAR- γ activity: molecular aspects related to obesity and side-effects. *PPAR Res* 2007: 32696.

Zhang Y, Li R, Meng Y, Li S, Donelan W, Zhao Y *et al.* (2014). Irisin stimulates browning of white adipocytes through mitogen-activated protein kinase p38 MAP kinase and ERK MAP kinase signaling. *Diabetes* 63: 514–525.

Supporting Information

Additional Supporting Information may be found online in the supporting information tab for this article.

<https://doi.org/10.1111/bph.14139>

Figure S1 The chemical structure of the natural compounds formononetin and calycosin.

Figure S2 The HPLC analysis of the water extract of *Astragalus membranaceus* (A) and formononetin (B).

Figure S3 The UCP1 expression was detected in the inguinal adipose tissues. Western blot analysis of UCP1 in the inguinal white adipose tissue (iWAT, A) and densitometric analysis of the relative abundance of UCP1 (B) ($n = 5$), β -actin was adopted as an internal standard to control for unwanted sources of variation, the ratio of UCP-1 expression in BAT was normalized to β -actin (control). Data represent mean \pm SEM, the experiments had been repeated three times, $*P < 0.05$.

Figure S4 Eight-week-old C57BL/6 J male mice were fed a high fat diet for 8 weeks to become obese and then treated with the vehicle or formononetin for 8 weeks, followed by analysis of (A) CO₂ production, (B) activity. ($n = 5$). Data represent mean \pm SEM, the experiments had been repeated three times, $*P < 0.05$.

Figure S5 Eight-week-old C57BL/6 J male mice were fed a high fat diet for 8 weeks to become obese and then treated with the vehicle (control) or formononetin for 8 weeks at thermoneutrality ($n = 6$ mice).

Figure S6 The synergistic effect of AhR inhibitor StemRegenin 1 (SR1) and formononetin on *Ucp1*'s expression ($n = 5$). For quantitative RT-PCR experiments, 18S ribosomal RNA was adopted as an internal standard to control for unwanted sources of variation. The *ucp1* gene's average mRNA expression was normalized to the blank control (baseline). Data represent mean \pm SEM, the experiments had been repeated three times, $*P < 0.05$.

Figure S7 Rosglitazone (A) and calycosin (B) dose dependently promoted luciferase activity in COS7 cells transfected with PPAR γ and PPRE-luciferase plasmids ($n = 5$). The luciferase activity was normalized to the blank control as baseline. Data represent mean \pm SEM, the experiments had been repeated three times, $*P < 0.05$.

Figure S8 The mRNA (A) and protein (B) expression of *Ppar γ* in siRNA knockdown of *Ppar γ* in primary inguinal adipocytes ($n = 5$). For quantitative RT-PCR experiments, 18S ribosomal RNA was adopted as an internal standard to control for unwanted sources of variation. The *Ppar γ* gene's average mRNA expression was normalized to the blank control (baseline). Data represent mean \pm SEM, the experiments had been repeated three times, $*P < 0.05$.

Figure S9 The liver tissue weight (left) and TG contents in liver (right) in control mice and formononetin treated mice ($n = 5$). Data represent mean \pm SEM, the experiments had been repeated three times, $*P < 0.05$.